

Supplement of Biogeosciences, 12, 1537–1559, 2015
<http://www.biogeosciences.net/12/1537/2015/>
doi:10.5194/bg-12-1537-2015-supplement
© Author(s) 2015. CC Attribution 3.0 License.



Supplement of

Organic carbon production, mineralisation and preservation on the Peruvian margin

A. W. Dale et al.

Correspondence to: A. W. Dale (adale@geomar.de)

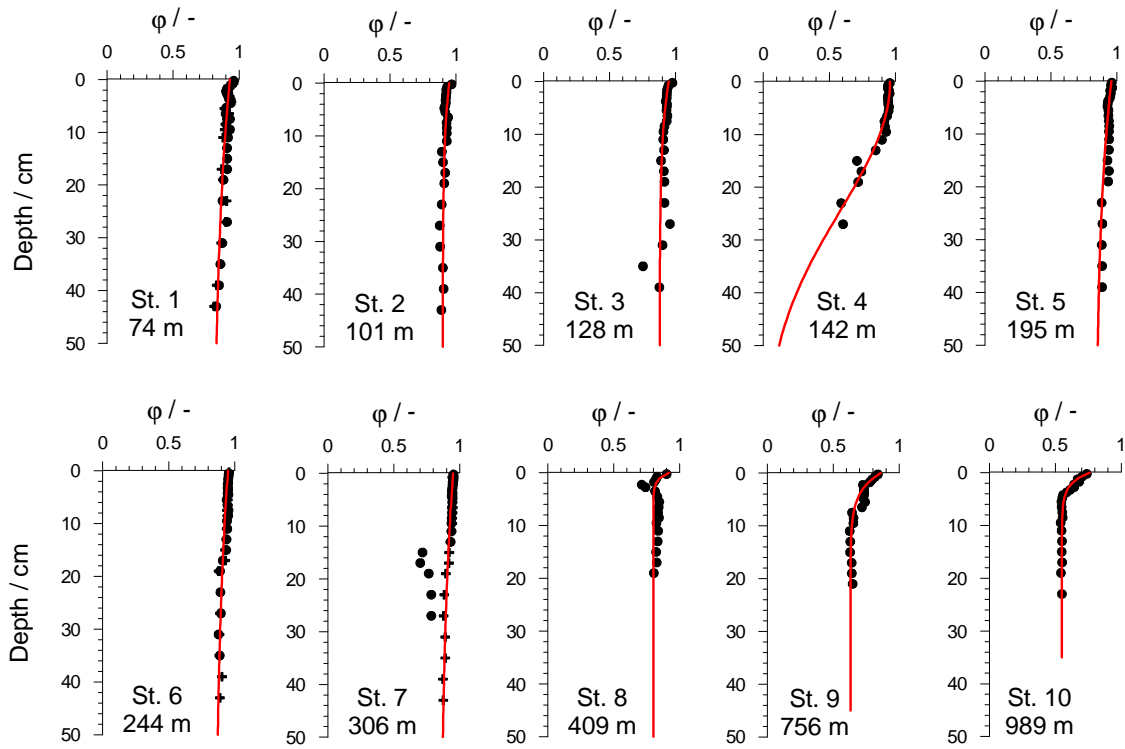


Figure S1. Measured (symbols) and modeled porosity at 12°S using the parameters listed in Table S2 (see Bohlen et al. (2011) for porosity parameters at 11°S). Data correspond to the multiple-cores (MUC) listed in Table 1 in the main text where different symbol types signify repeated coring at the same station.

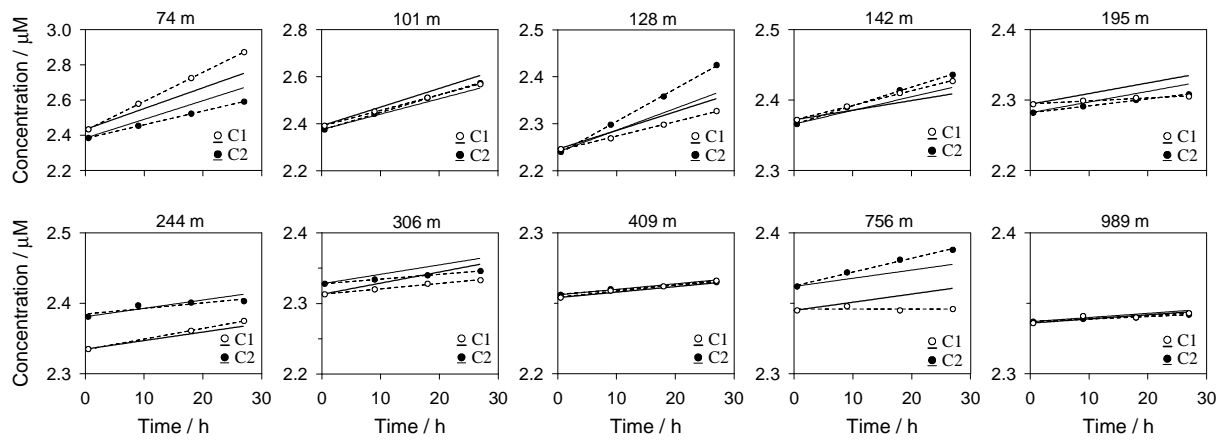


Figure S2. Dissolved inorganic carbon (DIC) concentrations inside the benthic chambers from 12°S (symbols). Open and filled circles refer to chamber 1 and 2, respectively. The dashed lines denote linear regression curves through the data from which the fluxes in Table 2 were calculated. The solid lines are the predicted changes in concentration using the DIC fluxes computed by the numerical model.

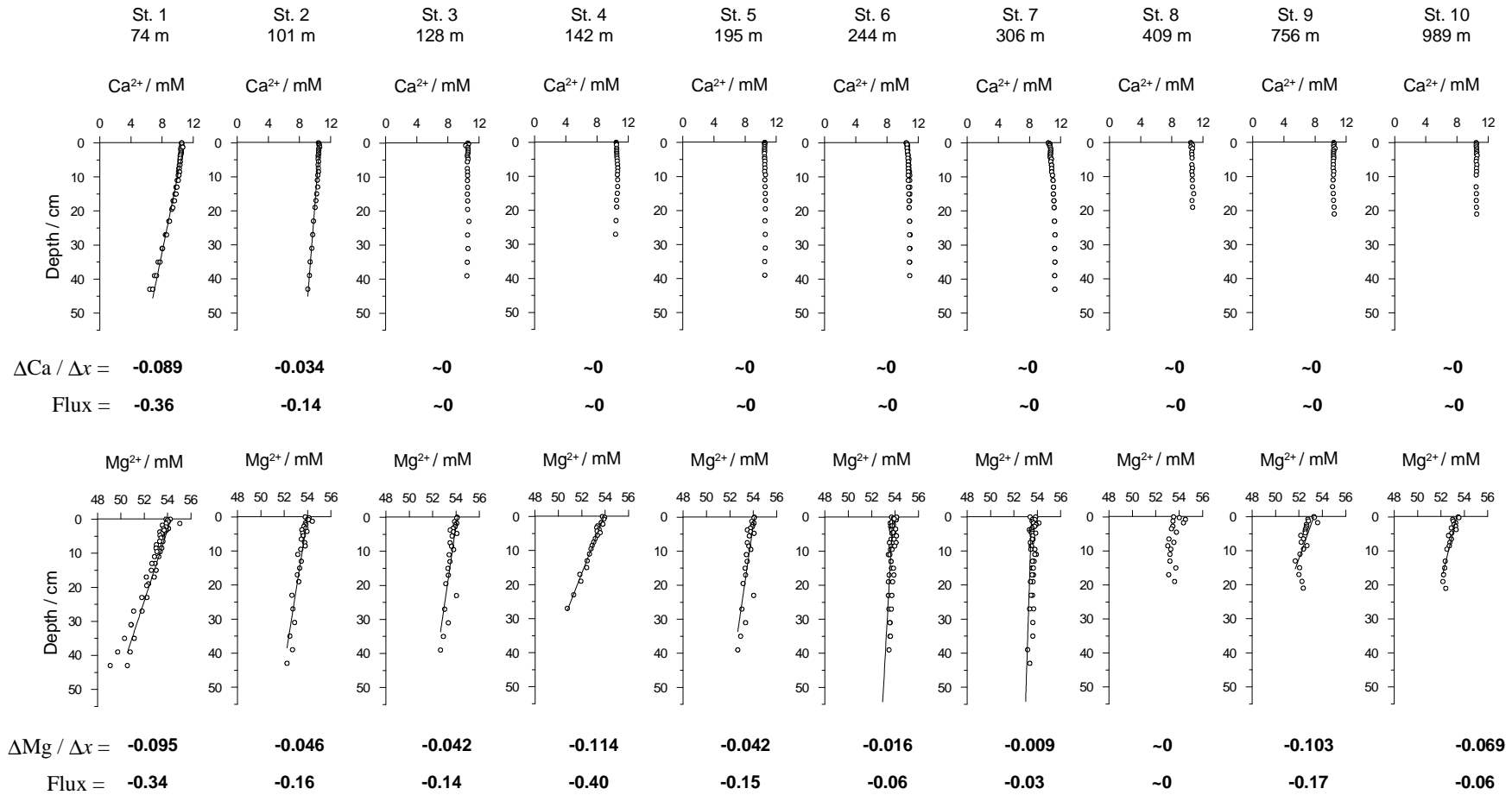


Figure S3. Dissolved porewater calcium (Ca^{2+}) and magnesium (Mg^{2+}) concentrations at 12°S . The solid lines denote linear regression curves where a concentration gradient ($\Delta\text{Ca}/\Delta x$, $\Delta\text{Mg}/\Delta x$) was apparent. The concentration gradients are given (in $\mu\text{mol cm}^{-4}$) from which the diffusive fluxes were calculated (in $\text{mmol m}^{-2} \text{d}^{-1}$) using Fick's First Law and diffusion coefficients corrected for site-specific tortuosity and temperature.

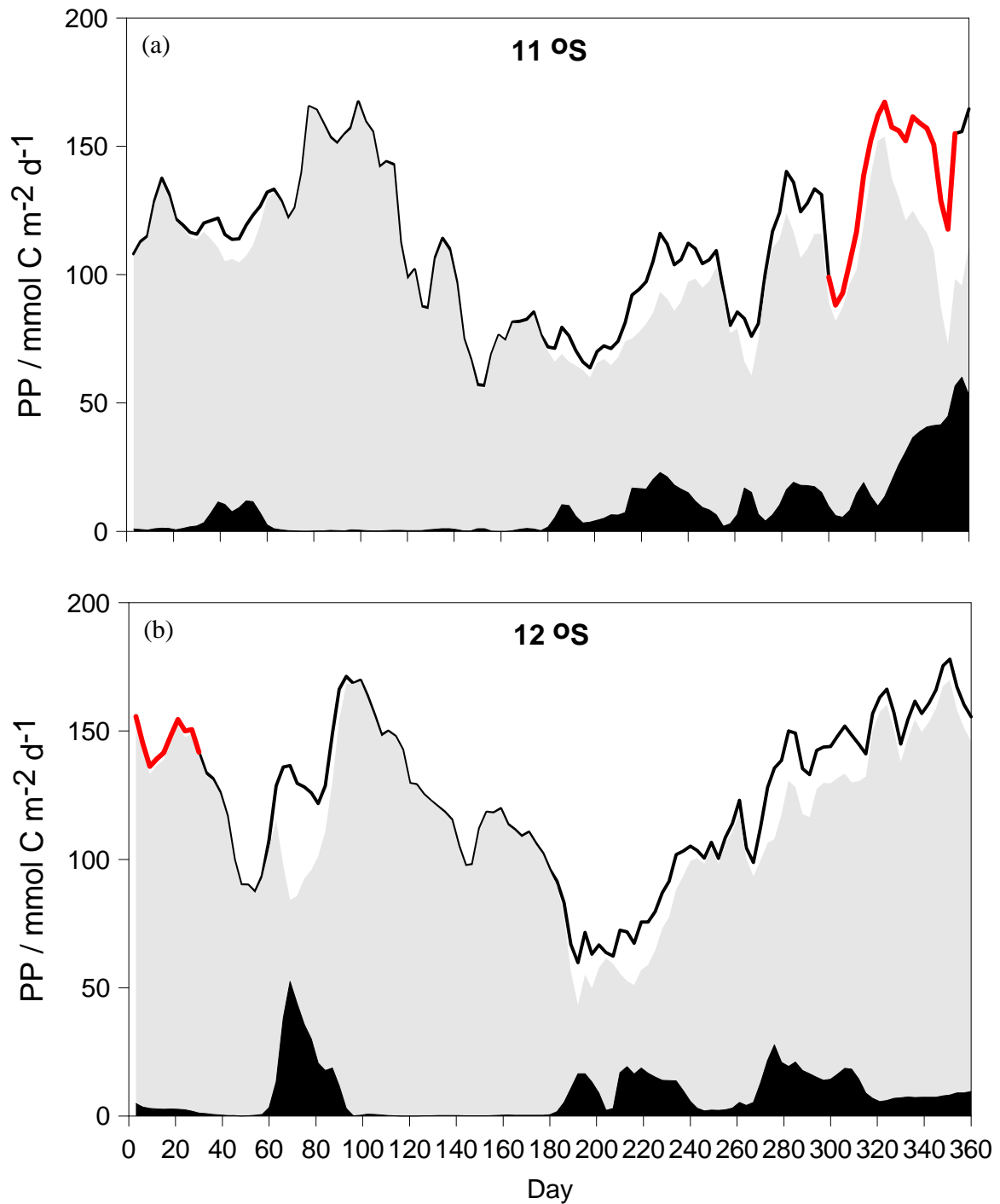


Figure S4. Three-day moving average primary production ($\text{mmol C m}^{-2} \text{d}^{-1}$) at ca. 100 m water depth on the 11 and 12 °S transects calculated by the ROMS-BioEBUS model (thick black line). The contribution from small and large phytoplankton groups are shown in black and grey, respectively. The red lines show the periods when the fieldwork was conducted.

Table S1. Measured TA and pCO₂ concentrations in the benthic chambers at 12°S. TA measured in the syringe samples was corrected for dilution by distilled water in the Vygon tubes (see main text) using the chloride concentration. Linear regression of the syringe samples was used to adjust TA to the times when the glass tubes samples were withdrawn for pCO₂ analysis. DIC was calculated as described in the main text. (C1 = chamber 1, C2 = chamber 2).

BIGO I-II (74 m)	Time syringes (h)	TA corrected (mM)	Time tubes (h)	TA (mM)	pCO ₂ (ppm)	DIC (μM)
C1_1	0.25	2.31	0.5	2.474	1402	2434
C1_2	4	2.57				
C1_3	8	2.70	9	2.631	1561	2579
C1_4	12	2.78				
C1_5	16	2.77	18	2.798	1654	2725
C1_6	20	2.88				
C1_7	24	2.86				
C1_8	28	2.92	27	2.964	1757	2872
C2_1	0.25	2.39	0.5	2.433	1367	2385
C2_2	4	2.45				
C2_3	8	2.55	9	2.510	1469	2454
C2_4	12	2.57				
C2_5	16	2.59	18	2.591	1550	2523
C2_6	20	2.59				
C2_7	24	2.58				
C2_8	28	2.72	27	2.672	1621	2591

BIGO I-V (101 m)	Time syringes (h)	TA corrected (mM)	Time tubes (h)	TA (mM)	pCO ₂ (ppm)	DIC (μM)
C1_1	0.25	2.46	0.5	2.450	1211	2391
C1_2	4	2.48				
C1_3	8	2.51	9	2.511	1285	2452
C1_4	12	2.48				
C1_5	16	2.60	18	2.576	1347	2511
C1_6	20	2.57				
C1_7	24	2.64				
C1_8	28	2.64	27	2.641	1399	2568
C2_1	0.25	2.36	0.5	2.434	1201	2375
C2_2	4	2.52				
C2_3	8	2.60	9	2.499	1274	2442
C2_4	12	2.46				
C2_5	16	2.48	18	2.569	1326	2509
C2_6	20	2.57				
C2_7	24	2.69				
C2_8	28	2.62	27	2.638	1366	2573

BIGO II-IV (128 m)	Time syringes (h)	TA corrected (mM)	Time tubes (h)	TA (mM)	pCO ₂ (ppm)	DIC (μM)
C1_1	0.25	2.24	0.5	2.287	1260	2246
C1_2	4	2.33				
C1_3	8	2.32	9	2.316	1223	2269
C1_4	12	2.42				
C1_5	16	2.42	18	2.346	1230	2298
C1_6	20	2.35				
C1_7	24	2.47				
C1_8	28	2.48	27	2.377	1275	2327
C2_1	0.25	2.35	0.5	2.276	1305	2240
C2_2	4	2.25				
C2_3	8	2.29	9	2.340	1287	2298
C2_4	12	2.31				
C2_5	16	2.30	18	2.408	1254	2358
C2_6	20	2.41				
C2_7	24	2.44				
C2_8	28	2.33	27	2.475	1301	2425

BIGO I-I (142 m)	Time syringes (h)	TA corrected (mM)	Time tubes (h)	TA (mM)	pCO ₂ (ppm)	DIC (μM)
C1_1	0.25	2.40	0.5	2.391	1570	2372
C1_2	4	2.43				
C1_3	8	2.39	9	2.404	1656	2391
C1_4	12	2.39				
C1_5	16	2.39	18	2.418	1719	2410
C1_6	20	2.41				
C1_7	24	2.40				
C1_8	28	2.48	27	2.431	1786	2427
C2_1	0.25	2.33	0.5	2.383	1594	2366
C2_2	4	2.41				
C2_3	8	2.49	9	2.399	1701	2390
C2_4	12	2.39				
C2_5	16	2.37	18	2.415	1808	2414
C2_6	20	2.40				
C2_7	24	2.41				
C2_8	28	2.47	27	2.431	1908	2436

BIGO I-IV (195 m)	Time syringes (h)	TA corrected (mM)	Time tubes (h)	TA (mM)	pCO ₂ (ppm)	DIC (μM)
C1_1	0.25	2.34	0.5	2.325	1366	2294
C1_2	4	2.31				
C1_3	8	2.33	9	2.325	1410	2299
C1_4	12	2.36				
C1_5	16	2.31	18	2.325	1459	2303
C1_6	20	2.31				
C1_7	24	2.31				
C1_8	28	2.32	27	2.325	1476	2305
C2_1	0.25	2.31	0.5	2.317	1319	2282
C2_2	4	2.32				
C2_3	8	2.37	9	2.324	1342	2291
C2_4	12	2.30				
C2_5	16	2.28	18	2.332	1351	2300
C2_6	20	2.32				
C2_7	24	2.37				
C2_8	28	2.34	27	2.340	1359	2308

BIGO II-II (244 m)	Time syringes (h)	TA corrected (mM)	Time tubes (h)	TA (mM)	pCO ₂ (ppm)	DIC (μM)
C1_1	0.25	2.39	0.5	2.371	1329	2335
C1_2	4	2.36				
C1_3	8	2.36	9			
C1_4	12	2.37				
C1_5	16	2.42	18	2.390	1407	2361
C1_6	20	2.38				
C1_7	24	2.41				
C1_8	28	2.39	27	2.400	1453	2375
C2_1	0.25	2.36	0.5	2.418	1338	2381
C2_2	4	2.48				
C2_3	8	2.47	9	2.418	1509	2397
C2_4	12	2.39				
C2_5	16	2.38	18	2.418	1551	2401
C2_6	20	2.42				
C2_7	24	2.45				
C2_8	28	2.40	27	2.418	1583	2403

BIGO II-I (306 m)	Time syringes (h)	TA corrected (mM)	Time tubes (h)	TA (mM)	pCO ₂ (ppm)	DIC (μM)
C1_1	0.25	2.44	0.5	2.367	1134	2313
C1_2	4	2.32				
C1_3	8	2.33	9	2.373	1153	2320
C1_4	12	2.37				
C1_5	16	2.37	18	2.379	1169	2328
C1_6	20	2.41				
C1_7	24	2.41				
C1_8	28	2.37	27	2.385	1169	2333
C2_1	0.25	2.39	0.5	2.385	1122	2328
C2_2	4	2.38				
C2_3	8	2.38	9	2.389	1143	2334
C2_4	12	2.41				
C2_5	16	2.40	18	2.393	1159	2340
C2_6	20	2.37				
C2_7	24	2.40				
C2_8	28	2.40	27	2.398	1173	2346

BIGO II-V (409 m)	Time syringes (h)	TA corrected (mM)	Time tubes (h)	TA (mM)	pCO ₂ (ppm)	DIC (μM)
C1_1	0.25	2.27	0.5	2.264	1367	2254
C1_2	4	2.27				
C1_3	8	2.30	9	2.266	1394	2259
C1_4	12	2.26				
C1_5	16	2.31	18	2.269	1401	2262
C1_6	20	2.34				
C1_7	24	2.37				
C1_8	28	2.29	27	2.272	1406	2266
C2_1	0.25	2.40	0.5	2.264	1387	2256
C2_2	4	2.26				
C2_3	8	2.45	9	2.266	1409	2260
C2_4	12	2.23				
C2_5	16	2.31	18			
C2_6	20	2.32				
C2_7	24	2.24				
C2_8	28	2.26	27	2.272	1398	2265

BIGO II-III (756 m)	Time syringes (h)	TA corrected (mM)	Time tubes (h)	TA (mM)	pCO ₂ (ppm)	DIC (μM)
C1_1	0.25	2.43	0.5	2.356	1138	2345
C1_2	4	2.32				
C1_3	8	2.41	9	2.356	1161	2348
C1_4	12	2.30				
C1_5	16	2.35	18	2.356	1139	2345
C1_6	20	2.34				
C1_7	24	2.37				
C1_8	28	2.33	27	2.356	1150	2346
C2_1	0.25	2.37	0.5	2.373	1144	2362
C2_2	4	2.38				
C2_3	8	2.33	9	2.381	1163	2372
C2_4	12	2.41				
C2_5	16	2.39	18	2.389	1175	2381
C2_6	20	2.40				
C2_7	24	2.45				
C2_8	28	2.34	27	2.397	1172	2388

BIGO I-III (989 m)	Time syringes (h)	TA corrected (mM)	Time tubes (h)	TA (mM)	pCO ₂ (ppm)	DIC (μM)
C1_1	0.25	2.32	0.5	2.357	1035	2336
C1_2	4	2.42				
C1_3	8	2.37	9	2.357	1077	2341
C1_4	12	2.34				
C1_5	16	2.32	18	2.357	1068	2340
C1_6	20	2.37				
C1_7	24	2.40				
C1_8	28	2.33	27	2.357	1091	2343
C2_1	0.25	2.31	0.5	2.357	1039	2337
C2_2	4	2.34				
C2_3	8	2.32	9	2.357	1056	2339
C2_4	12	2.37				
C2_5	16	2.36	18	2.357	1063	2340
C2_6	20	2.36				
C2_7	24	2.44				
C2_8	28	2.39	27	2.357	1081	2342

Table S2. Parameters and boundary conditions for simulating $^{210}\text{Pb}_{\text{xs}}$.

Description	St. 1 (74 m)	St. 2 (101 m)	St. 3 (128 m)	St. 4 ^a (142 m)	St. 5 (195 m)	St. 6 (244 m)	St. 7 (306 m)	St. 8 (409 m)	St. 9 (756 m)	St. 10 (989 m)
Dry sediment density, ρ (g cm^{-3})	2.0	2.0	2.0	2.0	2.0	2.0	2.0	2.0	2.0	2.0
Porosity at sediment surface (0 cm), $\varphi(0)$ (-)	0.93	0.95	0.95	0.96	0.96	0.95	0.95	0.92	0.86	0.76
Porosity at sediment base (L cm), $\varphi(L)$ (-)	0.80	0.90	0.88	-	0.84	0.87	0.85	0.80	0.63	0.55
Porosity attenuation length, z_{por} (cm)	0.03	0.1	0.10	-	0.04	0.03	0.03	0.90	0.30	0.50
Sediment accumulation rate, ω_{acc} (cm yr^{-1})	0.45	No $^{210}\text{Pb}_{\text{xs}}$ data	0.2	0.04	0.10	No $^{210}\text{Pb}_{\text{xs}}$ data	0.05	0.011	0.035	0.06
Bioturbation coefficient at sediment surface, $D_B(0)$ ($\text{cm}^2 \text{yr}^{-1}$)	1.0	No $^{210}\text{Pb}_{\text{xs}}$ data	4.0	2.0	1.0	No $^{210}\text{Pb}_{\text{xs}}$ data	0.5	0.05	0.1	0.1
Bioturbation halving depth, x_s (cm)	3.0	No $^{210}\text{Pb}_{\text{xs}}$ data	3.0	1.4	2.0	No $^{210}\text{Pb}_{\text{xs}}$ data	1.4	1.4	1.4	1.4
Flux of $^{210}\text{Pb}_{\text{xs}}$ to the sediment surface, $F(0)$ ($\text{Bq cm}^{-2} \text{yr}^{-1}$)	0.11	No $^{210}\text{Pb}_{\text{xs}}$ data	0.088	0.019	0.026	No $^{210}\text{Pb}_{\text{xs}}$ data	0.023	0.0016	0.025	0.015

^a Porosity at St. 4 (Figure S1) was better simulated using the function: $\varphi(x) = \varphi(0) \cdot \exp(-\frac{x^2}{1200})$